Sub-3 nm Particles Detection in a Large Photoreactor Background: Possible Implications for New Particles Formation Studies in a Smog Chamber

J. Boulon,[1] K. Sellegri,[1] Y. Katrib,[2] J. Wang,[2] K. Miet,[2] B. Langmann,[3] P. Laj,[4] and J.-F. Doussin[2]

[1]*Laboratoire de Météorologie Physique, Université Blaise Pascal, Aubière, France*
[2]*Laboratoire Inter-Universitaire des Systèmes Atmoshériques, Université Paris-Est, Créteil, France*
[3]*Institute of Geophysics, University of Hamburg, Germany*
[4]*Laboratoire de Glaciologie et Géophysique de l'Environnement, Université Joseph Fourier, Saint-Martin d'Héres, France*

New particles formation experiments have been conducted in the experimental multiphasic atmospheric simulation chamber (CESAM) smog chamber. The nucleation events generated during the dark ozonolysis of sabinene were monitored using a neutral cluster and air ions spectrometer in the size range 0.8–42 nm under simulated atmospheric conditions. The measurements show that a significant amount of pre-existing clusters exist in the 1–2 nm size range even in very clean controlled conditions. Numerical modeling experiments indicate that a range of 9–67% of pre-existing clusters can explain, through activation by organic vapors, the number of new particles formed when sabinene is oxidized, with an increasing contributing fraction for increasing condensable vapor concentrations. These findings suggest that atmospheric simulation chambers backgrounds have to be carefully characterized for their sub-3-nm neutral cluster concentration content before nucleation parameterizations can be derived.

1. INTRODUCTION

By acting as cloud condensation nuclei (CCN), aerosol significantly impacts the Earth radiative budget through the so-called aerosol indirect effects (Twomey 1974; Albrecht 1989). The number of new particles formed in the atmosphere by nucleation may contribute significantly to the total number concentrations burden and CCN concentrations at the global scale (Spracklen et al. 2006, 2010; Merikanto et al. 2009). Condensable organic gases are strongly suspected to participate to new

particle formation (NPF), at least in the early stages of growth (Fiedler et al., 2005; Laaksonen et al. 2008; Smith et al. 2008). However, the contribution of organic to the nucleation process itself still has remains unclear. Among volatile organic compounds, the terpene family is known to significantly contribute to the total fine particle burden from the local to the global scale (Pandis et al. 1991; Griffin et al. 1999; Kanakidou et al. 2005). Monoterpenes ($C_{10}H_{16}$), in particular α-pinene, β-pinene, sabinene, and limonene account for 40–80% of the overall terpene emission on a global scale, when isoprene is excluded. Their potential relevance as precursors of new particles has also been showed by different studies based on simulation chamber experiments and field measurements (Koch et al. 2000; Bonn et al. 2002; Rohr et al. 2003; Bonn et al. 2008). However, the nucleation events and the early steps of particles growth, which are commonly observed in the "seed-free" experiments are not well understood. Indeed, the critical concentrations needed to lead to nucleation for the least volatile products observed in these experiments are rarely reached. Authors have considered as possible candidate transient species (Lee and Kamens 2005) while some others (Metzger et al. 2010) invoke the formation of sulfuric acid-organic critical clusters. Thus, considerable uncertainty remains about the existence and significance of nucleation in chamber experiments.

A major factor behind this persistent activity is a lack of data on particles below 10-nm diameter in chamber studies. A few experiments have reported on particles as small as the detection limit of conventional condensation particle counters (CPCs), but even this small size is much larger than the initial nuclei. Only recently have instruments been developed that enable measurements of sub-3 nm particles with sufficient time resolution to probe the rapid changes in the size distribution that occur during nucleation events. Recent ambient measurements underline the critical importance of measurements (Sipilä et al.

2010; Jiang et al. 2011; Kuang et al. 2011). In the present work, we investigate the NPF derived from the sabinene ozonolysis in a laboratory smog chamber with a special focus on the nanoparticles background.

2. EXPERIMENTAL

2.1. Cluster Measurements

Recently, Mirme and Mirme 2011 developed a NAIS (i.e., neutral air ion and cluster spectrometer). This instrument, which has been extensively used for field measurements (Boulon et al. 2010, 2011; Manninen et al. 2010), provides charged and total particle size distribution (PSD) measurements from 0.8 to 42 nm in NTP-conditions. According to Asmi et al. (2009), the neutral particle measurements below 3 nm are not reliable at low particle concentrations. In the neutral mode, the NAIS uses a corona discharge to charge the atmospheric particles population to equilibrium. Doing so, it also produces a charged sub-3-nm cluster population. The internal production of these cluster ions is variable in time and strongly depends on environmental conditions. Therefore, the reliableness of sub-3 nm particles measurement is questionable especially in clean environments. In contrast, sub-3 nm cluster concentrations in chamber experiments may well be high enough, and background variability low enough to enable quantitative measurements of these small particles. Indeed, the number concentration of newly formed particles may exceed by far the usual sub-3 nm cluster population produced within the instrument due to corona effect (the term "self-produced" will be used hereafter to qualify those particles produced by a process peculiar to the NAIS). In consequence, a NAIS has been used to perform nanoparticles measurements from 0.8 to 42 nm in the CESAM chamber. It was connected to the simulation chamber using a 38-mm internal diameter copper pipe. Sampled air was drawn to the instrument at a flow rate of 60 lpm.

2.2. Simulation Chamber Experiments

Dark ozonolysis experiments of sabinene were carried out in the CESAM simulation chamber in a dry atmosphere (RH < 1%). The CESAM simulation chamber has been described in (Wang et al. 2011). It is made of stainless steel and has a 4.2-m^3 volume that allows a mixing time lower than a minute (∼45 s according to Wang et al. [2011]). The smog chamber is initially filled with 80% of N_2 and 20% of O_2. However, due to the high sampling flowrate of the NAIS, the chamber is continuously refilled by N_2 from a liquid nitrogen tank. All injection tubing is made of Teflon®; thus, preventing ions from being introduced in the chamber. One of the consequences of the refill procedure is that the N_2:O_2 ratio is a function of time. To avoid variation in the carrier gas composition, all the 26 experiments were conducted according to a very strict protocol. For all experiments, the chamber pressure and the ozone-mixing ratio at the time of injection were kept unchanged (1000 hPa, O_3 = 100 ppb, N_2:O_2 = 8.5 ± 0.4) while different initial terpene concentration

was injected (from 10 to 90 ppb). PSD for charged and neutral particles, were obtained with a time resolution of 2 min from NAIS measurements during a total reaction time of 40 min, in which the monoterpene was consumed by nearly 100%. In order to provide very clean conditions, the chamber was cleaned prior to each experiment using high ozone concentrations (few ppm) following by a strong vacuum of 10^{-7} atm to enhance wall material desorption.

2.3. Chemicals

Sabinene was purchased from Interchim (Montluçon, France). All runs were conducted in a synthetic air produced from the mixture of ca. 200 mbar of O_2 (Air Liquide®, Alphagaz® class 1) and ca. 800 mbar of nitrogen produced from liquid nitrogen kept at a pressure between 5 and 20 bar. This nitrogen source is economic but moreover it is virtually free from low volatility trace gases as it is freshly produced from the evaporation of N_2 which temperature ranges between 90 and 110 K (depending the tank pressure). Nevertheless, it must be indicated the nitrogen flow produced exhibits a contamination of carbon monoxide ranging from 0.1 to 1 ppm. Samples collected by passing this gas mixture through sorbent tubes were thermally desorbed into a gas chromatograph/mass spectrometry system for trace species analysis. No other significant contaminant was detected. Furthermore, the tubings between the tank and the chamber were always overpressurized to minimize any possible contamination from possible leaks. Additional experiments were performed replacing the nitrogen source with cylinders (Air Liquide®, Alphagaz® class 1).

3. RESULTS

3.1. Smog Chamber Background

Both charged and neutral particle formation were monitored by the NAIS. Previously to the terpene injection, the ion background concentration was in average 133 ± 34 #.cm^{-3} and 166 ± 30 #.cm^{-3}, respectively for positive and negative ions, which is in the low range of production by galactic cosmic rays (1100−4300 cm^{-3} assuming an equilibrium ion-pair concentration and in absence of any losses except ion–ion recombination and a production rate ∼2−30 #. cm^{-3}.s^{-1}), confirming that no ions were introduced in the system. During NPF events, the contribution of the charged fraction was measured to be lower than 1% suggesting that no ion-induced reactions were involved. Consequently, only results involving neutral particle will be presented in the following.

Surprisingly, a sub-3 nm cluster population was detected inside the chamber at high concentrations during the whole duration of the experiments. Aware of the Asmi et al. (2009) warning about NAIS neutral sub-3 nm cluster "self-produced" population, we produced by the NAIS for a given thermodynamical conditions set could be estimated by in stalling a filter in-between the smog chamber sampling outlet and the NAIS inlet thus filtering the air sucked by the instrument. The analysis
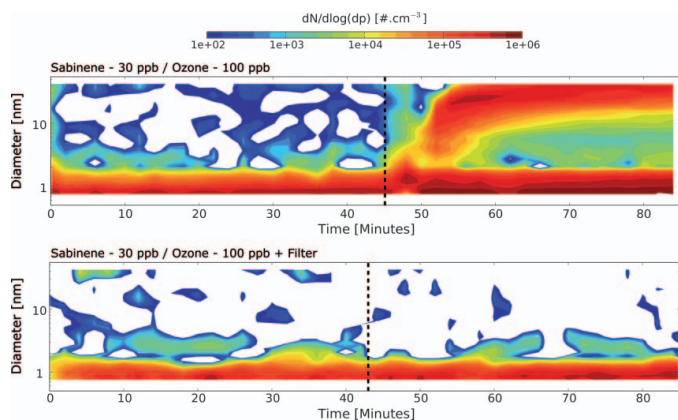
FIG. 1.   Total particle size distribution measurements during sabinene ozonolysis (sabinene = 30 ppb and ozone = 100 ppb) without filter (upper panel) and using a particle filter (bottom panel). The sabinene injection is indicated by the black dotted line. (Color figure available online.)

of the fraction of particles which are still detected by the instrument, provide the number of "self-produced" particles due to the corona effect inside the NAIS. The filter was built using gas-mask filters (MSA, "Advantage 200" P3) since their porosity allows for high flow rates such as the one needed for NAIS measurements. Filtered experiments were conducted both in blank conditions ($N_2 + O_2$ and O_3) and connected to the outlet of the CESAM chamber during a full ozonolysis experiment (Figure 1, lower panel). From ambient measurements, we calculated that the efficiency of such a filter on the PSD is on average 95% of charged particles concentration and 76% of the total particles (charged and neutral) concentration. The lower apparent filtering efficiency for total particles is due to the NAIS internal production of sub-3 nm ions during the neutralization phase (Asmi et al. 2009). Hence, for (T, P, RH) conditions of the ambient experiment (respectively $8.4 \pm 0.9°C$, 945 ± 0.5 hPa, and $63.7 \pm 4.5\%$ RH), the sub-3 nm particles generated inside the instrument was estimated to be respectively for positive and negative analyzer $\sim 2350 \pm 200$ and $\sim 5600 \pm 640$ #.cm^{-3}. A recent paper by Manninen et al. (2011) shows that the number and chemical composition of such ions is strongly influenced by the carrier gas composition. To evaluate this effect, we also conducted filtered experiment during a full sabinene ozonolysis experiments (Figure 1, lower panel). These measurements provide an upper limit for the NAIS cluster "self-production" of $52 \pm 4.8 \times 10^{+03}$ #.cm^{-3}. This value is statistically identical to the one found using the same filtering set-up but without sabinene injection, suggesting that the volatile organic compounds do not contribute to increase the instrumental signal noise through homogeneous nucleation inside the instrument. The estimated sub-3 nm "self-production" value can then be compared to the total cluster concentration measured in the CESAM chamber at the beginning of each experiment: $230 \pm 70 \times 10^{+03}$ #.cm^{-3} on average. As this value is significantly higher than the "self-produced" cluster population we had to conclude that the clus-

ters observed in the 1–2 nm range in the simulation chambers was truly representative of the chamber background. In addition, it is important to note that the experiments were conducted over two years, depending on the smog chamber availability, and that those clusters were detected during each experiments along the whole "experimental campaign."

3.2.   New Particle Formation Events

An example of a NPF event is reported on Figure 1 (upper panel). The observed nucleation events present a similar shape to the one observed in the nature, the so-called "banana shape." As already mentioned, we also observed a sub-3 nm cluster population present at high concentrations throughout the experiments. For each NPF experiment, we have calculated the 3 nm particle formation rate (J_3, in such experiments $J_3 \approx dN_{3nm}/dt$).

The potential impact of the pre-existing clusters on the NPF events was first investigated by analyzing the their impact on the formation rate J_3 for different condensable vapor concentration. This values are reported in Figure 2. The impact of the pre-existing cluster population is not obvious since the data set for a given injected sabinene concentration is not extensive.

However, for a given condensable vapor concentration, an increase in the pre-existing cluster concentration seems to enhance the 3 nm particle formation rate. Although this conclusion
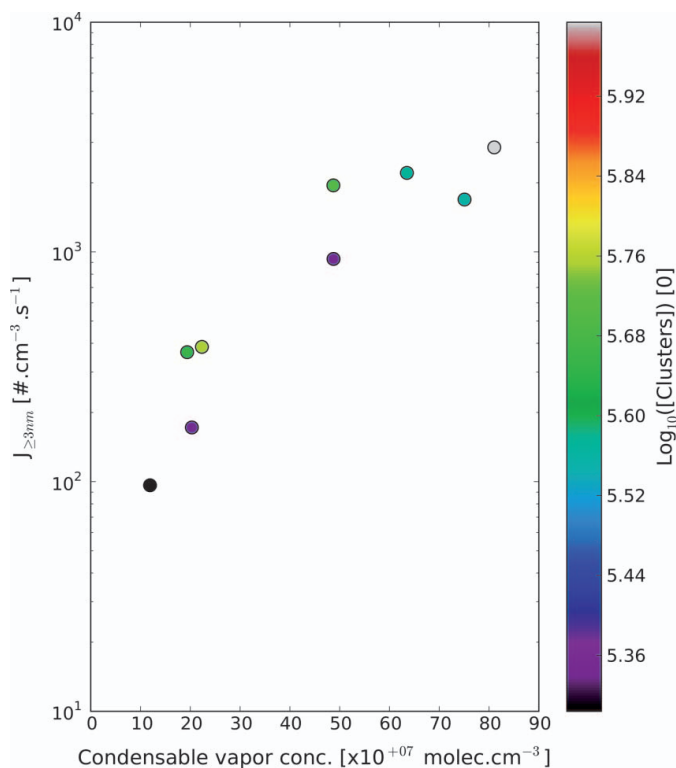

FIG. 2.   Variation in the calculated 3 nm particle formation rate according to the condensable vapor concentration and the pre-existing cluster population. (Color figure available online.)

is based on very few data, it suggests that the pre-existing cluster contribution might be stronger at lower condensable vapor concentrations. In order to infer whether or not observed pre-existing clusters play a role in our experiments, NPF numerical simulations were performed. Simulations where conducted to answer the following question: "Assuming there is not homogeneous nucleation from sabinene oxidative products, how many pre-existing clusters are needed to explain such NPF events?"

3.3.   Numerical Simulation

The NPF events were simulated using a simplified version of the M7 model (Vignati et al. 2004) developed for such experiments. This simple model, named M4-NPF, works as follow: given an initial cluster population source rate and condensable vapor concentration the model computes the evolution of the PSD according to condensation and coagulation processes from M7. In these simulations, we assumed (1) that only one "mean compound" is condensing on a pre-existing seed population, (2) the newly formed aerosols are not assumed to be liquid but viscous or solid (in agreement with Virtanen et al. 2010; Koop et al. 2011; Vaden et al. 2011), (3) aerosols are spherical. Also, the model is physical based only which mean that no molecular interactions from the chemical nature of compounds were accounted for. Consequently, from assumption 2, the evaporation term of the condensation equation becomes negligible. Hence, no surface tension risky estimation from the capillarity approximation is needed. Furthermore, in this context, the sticking coefficient is restricted to be a simple proportionality constant accounting for the effective quantity of vapor available for condensation. In this work, we supposed that this coefficient is equal to unity. Thus, from all those assumptions, it comes that we assume the growth to be a non-equilibrium process. This later point have been recently studied and is supported by the work of Perraud et al. (2012).

Particles are considered soluble and neutral and are distributed over 5 size bins (0–3; 3–10; 10–30 nm; 30–100 nm, and above). The condensable vapor molecular mass and
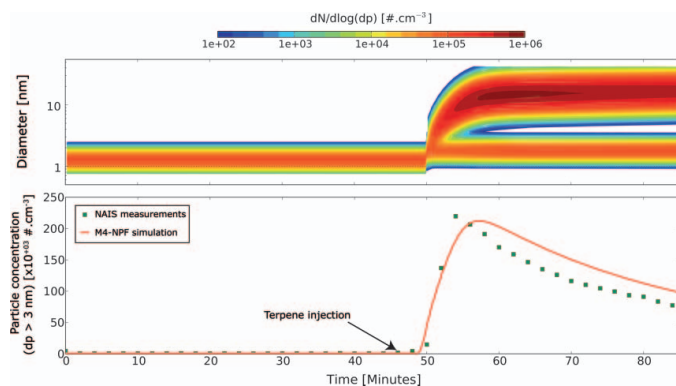

FIG. 3.   Simulated total particle size distribution (upper panel) and concentration (bottom panel) of a sabinene ozonolysis (sabinene = 30 ppb and ozone = 100 ppb). The data are represented in black squares while the simuation output is the black line. (Color figure available online.)

concentration are respectively derived from the work of Müller et al. (2009) and from growth rates calculated according to the procedure of Nieminen et al. (2010). The vapor diffusion coefficient was derived using the methodology proposed by Poling et al. (2001). Constrained by the measured total particle concentration, the model outputs the optimal cluster population needed to explain the observed growth and particle concentration (Figure 3). For sabinene concentration greater than 30 ppb, the growth transient is very fast and the particle size reaches the upper detection limit of the NAIS very quickly. Consequently, the numerical simulations were conducted on the smallest concentrations (i.e., 10 and 30 ppbv). We compare the fraction of activated clusters found by the model for 10 and 30 ppbv experiments with similar measured pre-existing cluster concentration, respectively 2.2 and 2.0 $\times$ 10^{+05} #.cm^{-3}. It was estimated that the fraction of activated clusters was 57% for 30 ppb experiment while the fraction falls down to 15% when 10 ppb sabinene is injected. We found that the simulation results are highly sensitive to the vapor properties (mass, diffusion coefficient) and taking into account this sensitivity, the optimal cluster activated fraction for 10 and 30 ppb experiments are respectively 17 $\pm$ 8% and 56 $\pm$ 10%.

4.   DISCUSSION AND CONCLUSIONS

Sabinene dark ozonolysis experiments were conducted in the CESAM smog chamber. NPF events derived from those chemical reactions were detected and monitored using a NAIS. Even though the smog chamber was consciously cleaned before experiments, high number concentration of neutral sub-3 nm particle (230 $\pm$ 70) $\times$ 10^{+03} #.cm^{-3} were measured within the chamber. It is also important to note that those experiment were conducted over two years thus the contamination hypothesis can be rejected. A direct correlation between pre-existing cluster concentrations and number of particles formed during the experiments were not shown to be obvious from direct measurements due to our restricted dataset. However, concentrations of pre-existing clusters are so high that there is the possibility that only of fraction of them are activated to new particles when condensable vapors are produced. This fraction is dependant on the condensable vapors available for condensational growth. This hypothesis was tested using numerical simulations. NPF simulations support the assumption that those pre-existing clusters may contribute to NPF in smog chamber experiments since heterogeneous nucleation on a fraction of those clusters can account for the observed events. The optimal cluster concentration was found to vary between 9% and be 66% of the concentrations derived from NAIS measurement, depending on the condensable vapors available. However, these results are not excluding the possibility the pre-existing clusters are not participating to the NPF formation at all, and that nucleation is still occurring in the chamber from the sabinene oxidation products only. Moreover, we were not able to clearly identify the origin of the observed cluster population and cross testing procedure using

different instruments are needed to further discuss the clusters' origin. Despite this, our results suggest that the smog chamber background should be accurately investigated prior performing nucleation and growth experiments. Indeed, those pre-existing cluster might introduce a bias in our understanding of the first steps of the NPF by by-passing the homogeneous nucleation process during nucleation experiments. Therefore, we suggest to perform such sub-3 nm background measurement on different smog chambers using different instrumental techniques to clarify the potential origin and impact of such clusters on nucleation studies.

REFERENCES

Albrecht, B. (1989). Aerosols, Cloud Microphysics and Fractional Cloudiness. *Science*, 245:1227–1230.

Asmi, E., Sipilä, M., Manninen, H. E., Vanhanen, J., Lehtipalo, K., Gagné, S., et al. (2009). Results of the Frst Air Ion Spectrometer Calibration and Intercomparison Workshop. *Atmos. Chem. Phys.*, 9:141–154.

Bonn, B., Kulmala, M., Riipinen, I., Sihto, S.-L., and Ruuskanen, T. M. (2008). How Biogenic Terpenes Govern the Correlation between Sulfuric Acid Concentrations and New Particle Formation. *J. Geophys. Res.*, 113:D12209.

Bonn, B., Schuster, G., and Moortgat, G. K. (2002). Influence of Water Vapor on the Process of New Particle Formation During Monoterpene Ozonolysis. *J. Phys. Chem. A*, 106:2869–2881.

Boulon, J., Sellegri, K., Hervo, M., Picard, D., Pichon, J.-M., Fréville, P., et al. (2011). Investigation of Nucleation Events Vertical Extent: A Long Term Study at Two Different Altitude Sites. *Atmos. Chem. Phys.*, 11:5625–5639.

Boulon, J., Sellegri, K., Venzac, H., Picard, D., Weingartner, E., Wehrle, G., et al. (2010). New Particle Formation and Ultrafine Aerosol Climatology at a High Altitude Site in the Alps (Jungfraujoch, 3580m a.s.l., Switzerland). *Atmos. Chem. Phys.*, 10:9333–9349.

Fiedler, V., Dal Maso, M., Boy, M., Aufmhoff, H., Hoffmann, J., Schuck, T., et al. (2005). The Contribution of Sulfuric Acid to Atmospheric Particle Formation and Growth: A Comparison between Boundary Layers in Northern and Central Europe. *Atmos. Chem. Phys.*, 5:1773–1785.

Griffin, R. J., Cocker, D. R., Flagan, R. C., and Seinfeld, J. H. (1999). Organic Aerosol Formation from the Oxidation of Biogenic Hydrocarbons. *J. Geophys. Res.*, 104(D3):2555–3567.

Jiang, J., Zhao, J., Chen, M., Eisele, F. L., Scheckman, J., Williams, B. J., et al. (2011). First Measurements of Neutral Atmospheric Cluster and 1–2 nm Particle Number Size Distributions During Nucleation Events. *Aerosol Sci. Technol.*, 45:ii–v.

Kanakidou, M., Seinfeld, J. H., Pandis, S. N., Barnes, I., Dentener, F. J., Facchini, M. C., et al. (2005). Organic Aerosol and Global Climate Modelling: A Review. *Atmos. Chem. Phys.*, 5:1053–1123.

Koch, S., Winterhalter, R., Uherek, E., Kolloff, A., Neeb, P., and Moortgat, G. K. (2000). Formation of New Particles in the Gas-Phase Ozonolysis of Monoterpenes. *Atm. Env.*, 34:4031–4042.

Koop, T., Bookhold, J., Shiraiwa, M., and Pöschl, U. (2011). Glass Transition and Phase State of Organic Compounds: Dependency on Molecular Properties and Implications for Secondary Organic Aerosols in the Atmosphere. *Phys. Chem. Chem. Phys.*, 13:19238–19255.

Kuang, C., Chen, M., Zhao, J., Smith, J., McMurry, P. H., and Wang, J. (2011). First Sizedependent Growth Rate Measurements of 1 to 5 nm Freshly Formed Atmospheric Nuclei. *Atmos. Chem. Phys.*, 12:3573–3589.

Laaksonen, A., Kulmala, M., O'Dowd, C. D., Joutsensaari, J., Vaattovaara, P., Mikkonen, S., et al. (2008). The Role of VOC Oxidation Products in Continental New Particle Formation. *Atmos. Chem. Phys.*, 8:2657–2665.

Lee, S., and Kamens, R. M. (2005). Particle Nucleation from the Reaction of α-Pinene and O_3. *Atm. Env.*, 39:6822–6832.

Manninen, H. E., Franchin, A., Schobesberger, S., Hirsikko, A., Hakala, J., Skromulis, A., et al. (2011). Characterization of Corona-Generated Ions Used in a Neutral Cluster and Air Ion Spectrometer (NAIS). *Atmos. Meas. Tech. Discuss.*, 4:2099–2125.

Manninen, H. E., Nieminen, T., Asmi, E., Gagné, S., Häkkinen, S., Lehtipalo, K., et al. (2010). EUCAARI Ion Spectrometer Measurements at 12 European Sites–Analysis of New Particle Formation Events. *Atmos. Chem. Phys.*, 10:7907–7927.

Merikanto, J., Spracklen, D. V., Mann, G. W., Pickering, S. J., and Carslaw, K. S. (2009). Impact of Nucleation on Global ccn. *Atmos. Chem. Phys.*, 9:8601–8616.

Metzger, A., Verheggen, B., Dommen, J., Duplissy, J., Prevot, A. S., Weingartner, E., et al. (2010). Evidence for the Role of Organics in Aerosol Particle Formation Under Atmospheric Conditions. *P. Natl. Acad. Sci. USA*, 107:6646–6651.

Mirme, S., and Mirme, A. (2011). The Mathematical Principles and Design of the NAIS -a Spectrometer for the Measurement of Cluster Ion and Nanometer Aerosol Size Distributions. *Atmos. Meas. Tech. Discuss.*, 4:7405–7434.

Müller, L., Reining, M.-C., Hayen, H., and Hoffmann, T. (2009). Characterization of Oligomeric Compounds in Secondary Organic Aerosol Using Liquid Chromatography Coupled to Electrospray Ionization Fourier Transform Ion Cyclotron Resonance Mass Spectrometry. *Rapid Commun. Mass Spectrom.*, 23:971–979.

Nieminen, T., Paasonen, P., Manninen, H. E., Kerminen, V.-M., and Kulmala, M. (2010). Parameterization of Ion-Induced Nucleation Rates Based on Ambient Observations. *Atmos. Chem. Phys.*, 10:21697–21720.

Pandis, S. N., Paulson, S. E., Seinfeld, J. H., and Flagan, R. C. (1991). Aerosol Formation in the Photooxidation of Isoprene and Beta-Pinene. *Atm. Env.*, 25:997–1008.

Perraud, V., Bruns, E. A., Ezell, M. J., Johnson, S. N., Yu, Y., Alexander, M. L., et al. (2012). Non Equilibrium Atmospheric Secondary Organic Aerosol Formation and Growth. *P. Natl. Acad. Sci. USA*, 109:2836–41.

Poling, B. E., Prausnitz, J. M., and O'Connel, J. P. (2001). *The Properties of Gases and Liquids,* 5th ed., McGraw-Hill Professional, New York.

Rohr, A. C., Weschler, C. J., Koutrakis, P., and Spengler, J. D. (2003). Generation and Quantification of Ultrafine Particles Through Terpene/Ozone Reaction in a Chamber Setting. *Aerosol Sci. Technol.*, 37:65–78.

Sipilä, M., Berndt, T., Petäjä, T., Brus, D., Vanhanen, J., Stratmann, F., et al. (2010). The Role of Sulfuric Acid in Atmospheric Nucleation. *Science*, 327:1243–1246.

Smith, J. N., Dunn, M. J., VanReken, T. M., Iida, K., Stolzenburg, M. R., McMurry, P. H., et al. (2008). Chemical Composition of Atmospheric Nanoparticles Formed from Nucleation in Tecamac, Mexico: Evidence for an Important Role for Organic Species in Nanoparticle Growth. *Geophys. Res. Lett.*, 35:1–5.

Spracklen, D. V., Carslaw, K. S., Kulmala, M., Kerminen, V.-M., Mann, G. W., and Sihto, S.-L. (2006). The Contribution of Boundary Layer Nucleation Events to Total Particle Concentrations on Regional and Global Scales. *Atmos. Chem. Phys.*, 6:5631–5648.

Spracklen, D. V., Carslaw, K. S., Merikanto, J., Mann, G. W., Reddington, C. L., Pickering, S., et al. (2010). Explaining Global Surface Aerosol Number Concentrations in Terms of Primary Emissions and Particle Formation. *Atmos. Chem. Phys.*, 10:4775–4793.

Twomey, S. (1974). Pollution and Planetary Albedo. *Atm. Env.*, 8:1251–1256.

Vaden, T. D., Imre, D., Beránek, J., Shrivastava, M., and Zelenyuk, A. (2011). Evaporation Kinetics and Phase of Laboratory and Ambient Secondary Organic Aerosol. *P. Natl. Acad. Sci. USA*, 108(6):2190–2195.

Vignati, E., Wilson, J., and Stier, P. (2004). M7: An Efficient Size-Resolved Aerosol Microphysics Module for Large-Scale Aerosol Transport Models. *J. Geophys. Res.*, 109:D22202.

Virtanen, A., Joutsensaari, J., Koop, T., Kannosto, J., Yli-Pirilä, P., Leskinen, J., et al. (2010). An Amorphous Solid State of Biogenic Secondary Organic Aerosol Particles. *Nature*, 467:824–827.

Wang, J., Doussin, J.-F., Perrier, S., Perraudin, E., Katrib, Y., Pangui, E., et al. (2011). Design of a New Multi-Phase Experimental Simulation Chamber for Atmospheric Photosmog, Aerosol and Cloud Chemistry Research. *Atmos. Meas. Tech. Discuss*, 4:315–384.